Atmospheric Pollution Research 16 (2025) 102527

Contents lists available at ScienceDirect

Atmospheric Pollution Research

journal homepage: www.elsevier.com/locate/apr

Long term (2011–2023) analysis of traffic and biomass burning contributions to black carbon in the third largest metropolitan area of Spain

Violeta Matos [a,*], Mar Sorribas [b], Sara Segura [a], María Pilar Utrillas [a], Víctor Estellés [a]

[a] Solar Radiation Group (GRSV), Department of Earth Physics and Thermodynamics, Universitat de València, Carrer Doctor Moliner, 50, Burjassot, 46100, Valencia, Spain

[b] Atmospheric Sounding Station – El Arenosillo, Atmospheric Research and Instrumentation Branch, INTA, Crta. San Juan del Puerto- Matalascañas, km 34, Mazagón, 21130, Huelva, Spain

ARTICLE INFO

Keywords:
Urban pollution
Absorbing aerosols
Equivalent black carbon
Source apportionment
Mann–Kendall test

ABSTRACT

This work is focused on the temporal characterization of equivalent Black Carbon (eBC) mass concentrations and their sources in a suburban station notably impacted by traffic, located in the metropolitan area of Valencia, Spain (western Mediterranean Sea). The average (± standard deviation) concentrations of fossil fuel (eBC_{ff}) and biomass burning (eBC_{bb}) contributions were 0.9 ± 0.5 μgm^{-3} and 0.06 ± 0.05 μgm^{-3}, respectively. These values represent the anthropogenic character of local aerosols. Both contributions also show a very marked seasonality: higher values in winter and lower in summer, corresponding to the strong dependence of the atmospheric conditions. The eBC_{ff} concentrations exhibit a daily pattern consistent with the evolution of traffic: a morning peak (around 8 LT) and other in the evening (around 19 LT). The seasonal Mann–Kendall test was applied to identify long-term trends and the Sen slope estimation to quantify the annual variation. Decreasing trends were found for eBC_{ff} concentrations (−0.023 μgm^{-3}/yr), showing the effectiveness of air quality regulations. Less noticeable trends were found for eBC_{bb} concentrations. This fact evidences the contribution of biomass burning is not only related to changes in anthropogenic emissions, but also to natural phenomena, making it more difficult to interpret long-term trends.

1. Introduction

According to the World Health Organization (WHO), around 99% of the world's entire population is exposed to air exceeding the guidelines and containing too high levels of some pollutants (WHO, 2013). On the other hand, anthropogenic aerosols play a major role in the observed changes in the climate system over the last decades. Certain air pollutants are currently regulated by a set of EU directives. The Ambient Air Quality Directives (AAQD) and other legislative frameworks aim to avoid, prevent, or reduce harmful effects on human health and the environment by keeping pollution levels across the EU within air quality standards. WHO (2021). To adhere to the WHO's latest targets, AAQD will include unregulated air pollutants, such as ultrafine particles (UFP), Black Carbon (BC) and ammonia (NH_3) (Council of the European Union, 2023). The climate and health effects of these pollutants are well known, making them *pollutants of emerging concern*.

BC has emerged as one of the most significant light-absorbing particulate components in the atmosphere. It represents a distinct fraction of carbonaceous aerosols, characterized by unique physicochemical properties. The characterization of BC aerosols is important because they play a key role in the terrestrial climate system and local air quality, especially in urban environments. The climate effects of BC aerosols are related to its strong absorption of light at all wavelengths of the visible spectrum, in addition to its resistance to chemical transformations (Bond et al., 2013). Other effects on the climate system are related to the formation and modification of clouds properties processes, the perturbation of the atmospheric temperature profile and the melting of snow and ice sheets, affecting the terrestrial albedo (Ding et al., 2016; Ji, 2016; Lee et al., 2017; Kang et al., 2020). BC aerosols are also associated with health effects, mainly related to increases in premature mortality from cardiovascular and respiratory diseases and lung cancer (Ljungman et al., 2019; Farzad et al., 2020). Much of the adverse health effects related to BC aerosols are caused, in large part, because of carbonaceous material such as semivolatile organic compounds and Polycyclic Aromatic Hydrocarbon (PAH) are adsorbed onto BC's core (Grahame et al., 2014).

Typically, BC particles are found in mixtures with other chemical compounds, many of which are co-emitted by a wide variety of sources. The formation of BC occurs during the combustion processes of fossil

* Corresponding author.
E-mail address: violeta.matos@uv.es (V. Matos).

https://doi.org/10.1016/j.apr.2025.102527
Received 25 October 2024; Received in revised form 28 March 2025; Accepted 30 March 2025
Available online 10 April 2025

and non-fossil carbonaceous fuels. Consequently, the study of BC is typically associated with analyzing the contributions of traffic and biomass burning, as they represent the most common sources in urban, rural and residential areas across Europe (Healy et al., 2017; Zotter et al., 2017; Mbengue et al., 2020; Savadkoohi et al., 2023). However, the presence of BC is also significant in port and industrial areas (Marín et al., 2017; Brewer, 2020).

In recent years, there has been a lack of consensus on the appropriate terminology for BC, considering all aspects of the properties, measurements methods, and associated uncertainties (Petzold et al., 2013; Lack et al., 2013) . Essentially, the terminology is linked to the measurement method, with “BC” serving as a qualitative term and “eBC” referring to the mass concentration of BC derived from the absorption coefficients (b_{abs}) obtained through optical methods. Instruments such as aethalometers, which conduct spectral measurements of b_{abs}, enable the source apportionment quantifying the contribution from fossil fuels and biomass burning to the total eBC. The source apportionment analysis is particularly pertinent in locations where emission sources are well defined, such as urban and metropolitan areas (Healy et al., 2017; Helin et al., 2018; Herich et al., 2011; Cheng et al., 2022; Savadkoohi et al., 2023), but also in residential zones and in regional backgrounds, where the biomass burning contribution is predominant (Helin et al., 2018; Mbengue et al., 2020).

The recent incorporation of BC in European legislation requires a comprehensive understanding of its temporal behavior and patterns, as this knowledge is crucial for the development of effective pollution control strategies. The concentration of eBC usually exhibits a marked seasonal dependence, largely influenced by atmospheric conditions (Titos et al., 2017; Jing et al., 2019; Shen et al., 2021; Matos et al., 2025). Several studies have shown that eBC, particularly the fossil fuel fraction (eBC_{ff}), follows a distinct daily pattern closely linked to traffic variations. This pattern is especially pronounced in urban and suburban areas, where vehicular emissions are the dominant source, as observed in various European (Järvi et al., 2008; Luoma et al., 2021) and Spanish cities (Casquero-Vera et al., 2021; Savadkoohi et al., 2023). Conversely, rural and residential areas display moderate fluctuations, as eBC from biomass burning plays a more significant role, particularly in Central and Northern Europe where biomass combustion is widely used in domestic heating devices (woodstoves/heating system), especially during the weekend (Herich et al., 2011; Zotter et al., 2017; Helin et al., 2018; Mbengue et al., 2020).

Temporal trends in eBC concentrations have also been documented in recent years across Europe, as reported by Sun et al. (2020), Luoma et al. (2021), Savadkoohi et al. (2023) and Matos et al. (2025). These findings indicate a substantial decline in traffic-related eBC levels and slight increasing in biomass burning contribution (Mousavi et al., 2018; Savadkoohi et al., 2023). The reduction of eBC_{ff} agree with the reduction in gaseous pollutants and particulate matter observed over the last decades (Sicard et al., 2021), but also in aerosol radiative properties (Gupta et al., 2022; Collaud Coen et al., 2020a; Garcia-Suñer et al., 2023). This evidence underscores the necessity of continued monitoring of eBC concentrations and demonstrates the effectiveness of air quality policies.

This study is the first to characterize the long-term contributions of traffic (BC_{ff}) and biomass burning (eBC_{bb}) to the total eBC concentrations in the metropolitan area of Valencia, situated in the western Mediterranean Sea. By examining interannual, intraannual, seasonal, and daily time scales, a comprehensive temporal analysis is provided. Furthermore, the temporal trends of eBC components concentrations over the last 12 years using the seasonal Mann–Kendall test and Sen’s slope estimator are analyzed. This robust method identifies increasing or decreasing trends over time, highlighting the annual rate of change.

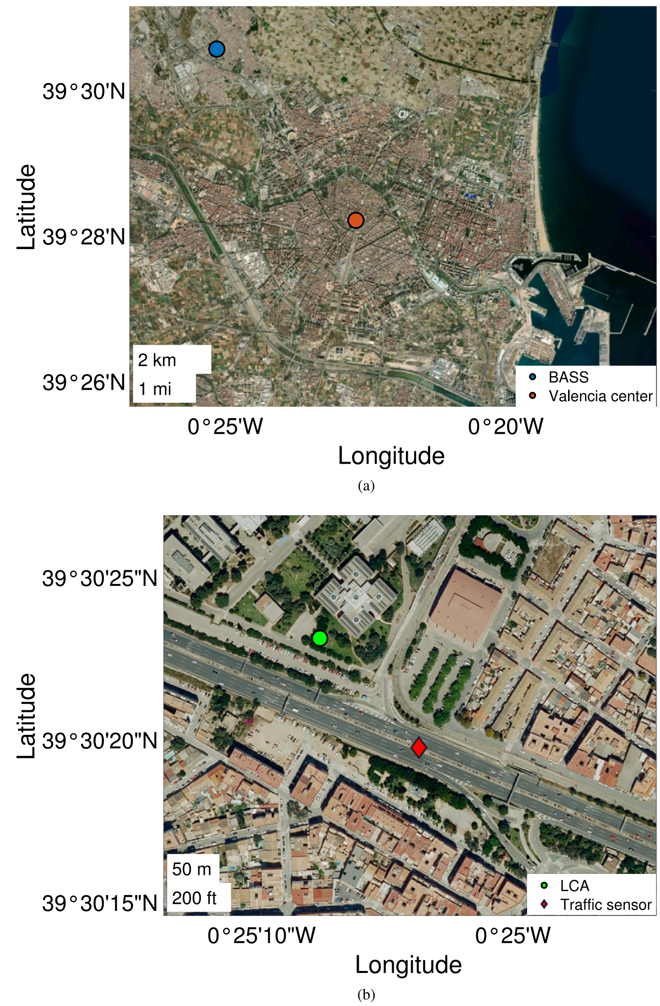

Fig. 1. Location of the measurement site: (a) BASS, Valencia center and Mediterranean Sea and (b) LCA location and traffic sensor.

2. Site description and instrumentation

2.1. Measurement site

Measurements used in this study were taken from the Atmospheric Pollution Laboratory (LCA, Laboratorio de Contaminación Ambiental), which is part of the Burjassot AtmoSpheric Station (BASS), located in the Burjassot Campus of the University of Valencia (39.51°N, 0.42°W, 60 m.a.s.l.).

Burjassot is a town located in the Metropolitan Area of Valencia (MAV), in the eastern coast of Spain (Fig. 1(a)). The population of Burjassot is 39,702 inhabitants, while in the MAV there are 1,599,656 inhabitants, from which 807,693 live in Valencia city. Burjassot is located 5 km northwest from Valencia city center and 10 km from the Mediterranean Sea.

The LCA is located near to a six-lane highway (CV-35), being one of the main roads leading to the center of Valencia. The traffic intensity of the CV-35 is high (more than 100k vehicles per day) especially during rush hours (approximately 14k vehicles from 7 to 8 Local Time, LT). Local authorities monitor the traffic intensity (expressed in number of vehicles per hour) in both ascending and descending directions (Fig. 1(b)). Although traffic is locally the main source of aerosols, the measurements are occasionally affected by particles transported from Sahara Desert, industrial areas of continental Europe or maritime and oceanic source regions (Esteve et al., 2012a). Additionally, they are often influenced by agricultural activities (such as burning of biomass debris, or resuspension of particles by soil preparation) (Estellés et al., 2005), as well as forest fires, primarily during summer (Gómez-Amo et al., 2017). Due to the location and anthropogenic influences, the LCA is considered a traffic suburban monitoring station.

2.2. Aethalometer AE31

An Aethalometer model AE31 (Magee Scientific) has been measuring from April 2011 to March 2023 at the LCA. The aethalometer is the most widely used filter-based instrument for real-time measurement of the b_{abs} and monitoring of the eBC mass concentrations.

The measurement principle is based on determining the attenuation measured by two photodetectors, one serving as a reference, while the filter continuously collects the aerosol samples. From the raw measurements of the two photodetectors, the beam attenuation (ATN) at a given time and for each wavelength can be derived. The attenuation coefficient, b_{atn}, is determined from the change in attenuation that the beam suffers during a time interval Δt:

$$b_{atn} = \left(\frac{ATN(\lambda, t + \Delta t) - ATN(\lambda, t)}{\Delta t} \right) \cdot \frac{A}{V} \tag{1}$$

where A represents the spot area (1.67 cm^2) and V is the flow rate (4 $L \cdot min^{-1}$). The b_{atn} differs from the b_{abs} due to three systematic artifacts, which need to be compensated: *loading*, *multiscattering* and *single scattering* effects. The compensation of these effects is based on different proposed algorithms: Weingartner et al. (2003), Arnott et al. (2005), Schmid et al. (2006), Virkkula et al. (2007) and Collaud Coen et al. (2010), although reference values that have been obtained in other works are usually used due to the inability to determine them experimentally.

The seasonal variations of the aerosol optical and radiative properties at this location, previously analyzed by Estellés et al. (2007), Esteve et al. (2012b) and Segura et al. (2016) require a specific-site compensation. In this work, the compensation proposed by Segura et al. (2014) is used, because the procedure is completely experimental and allows to obtain the spectral dependence of the parameters.

2.3. Atmospheric data

Meteorological variables (temperature, relative humidity, wind speed, pressure and precipitation) were monitoring with a Vaisala Weather Transmitter WXT520 sensor installed at BASS. This data were used to explain the seasonal behavior observed in the concentrations. Additionally, ERA5 reanalysis from ECMWF (European Centre for Medium-Range Weather Forecasts) (Hersbach et al., 2020) meteorological global model was used to obtain hourly data of the Boundary Layer Height (BLH), with a spatial resolution of 0.25°×0.25° (latitude × longitude).

3. Methodology

3.1. Compensation of the AE31 measurement

As mentioned above, raw measurements from the aethalometer allow the determination of the b_{atn} (Eq. (1)). Then, the b_{abs} is obtained by applying the following equation, which represents the compensation of the three effects suffered by the aethalometer measurements:

$$b_{abs}(\lambda) = \frac{b_{atn}(\lambda)}{C \cdot \left[\left(\frac{1}{f(\lambda)} - 1 \right) \cdot \frac{\ln(ATN(\lambda)) - \ln(10\%)}{\ln(50\%) - \ln(10\%)} + 1 \right]} \tag{2}$$

The shading factor, represented as *f*, is used to compensate for the loading effect. This factor was calculated for the seven wavelengths of the aethalometer, varying slightly from Weingartner et al. (2003) proposal. Basically, the dependence between the attenuation (ATN) and the b_{atn}, which appears when the aerosol loading deposited on the filter is high, was used. The values of b_{atn} before the filter advance should agree with the measurements made immediately after. The values of $f(\lambda)$ are selected by minimizing the differences between the values of the attenuation coefficient before and after filter advance (Sandradewi et al., 2008b; Favez et al., 2010; Segura et al., 2014; Matos et al., 2025).

The parameter *C* represents the enhancement of absorption by particles in the filter matrix due to multiple scattering. To obtain the values of $C(\lambda)$, the completely experimental approach proposed by Segura et al. (2014) and applied in Segura et al. (2016) and Matos et al. (2025) was used. This proposal arises from a combination of Weingartner et al. (2003) and Schmid et al. (2006) compensations methods. This proposal requires simultaneous complementary measurements of absorption and scattering coefficients: (a) for the measurements of reference absorption coefficients, a Multi-Angle Absorption Photometer (MAAP) Model 5012 was installed at the LCA from 2013 to 2015; (b) for the scattering coefficients, a TSI Model 3563 three-wavelength integrating nephelometer was used. The $C(\lambda)$ values obtained by Segura et al. (2016) at our measurement site were applied in this work. Both compensation parameters, f_λ and C_λ, are given in Table S1. For more detailed information on the compensation method, see Segura et al. (2014).

3.2. Fossil fuel and biomass burning contribution to eBC

The source apportionment of eBC methodology proposed by Sandradewi et al. (2008a), known as *Aethalometer Model* (hereafter AM), was used to quantify the relative contribution of eBC emitted from the burning of fossil fuel in traffic emissions (eBC_{ff}) and biomass burning (eBC_{bb}). This methodology has been widely used to analyze separately eBC contributions (Favez et al., 2010; Tiwari et al., 2014; Diaz Resquin et al., 2018; Mousavi et al., 2018, 2019; Mbengue et al., 2020; Cheng et al., 2022; Savadkoohi et al., 2023). The AM is based on the parameterization of the spectral dependence of b_{abs} of eBC emitted by both sources, assuming that the spectral dependence is different. Assuming that the total b_{abs} is only influenced by these two sources, the contributions from traffic and biomass burning can be determined by using:

$$b_{abs}(\lambda) = b_{abs}(\lambda)_{ff} + b_{abs}(\lambda)_{bb} \tag{3}$$

$$\frac{b_{abs}(\lambda_1)_{ff}}{b_{abs}(\lambda_2)_{ff}} = \left(\frac{\lambda_1}{\lambda_2} \right)^{-AAE_{ff}} \tag{4}$$

$$\frac{b_{abs}(\lambda_1)_{bb}}{b_{abs}(\lambda_2)_{bb}} = \left(\frac{\lambda_1}{\lambda_2} \right)^{-AAE_{bb}} \tag{5}$$

$$P = \frac{b_{abs}(\lambda_2)_{ff}}{b_{abs}(\lambda_2)} = \frac{eBC_{ff}}{eBC} \tag{6}$$

where λ_2 should be a wavelength in the N-IR range, where eBC is the main absorber, while λ_1 should be taken in the N-UV range, where other organic components also contribute to solar absorption. The most typical pair of values is 470–950 nm (Zotter et al., 2017), being identified as the optimal spectral selection for the application of the AM when using AE31 aethalometer measurements across Europe (Favez et al., 2010; Herich et al., 2011; Healy et al., 2017; Becerril-Valle et al., 2017; Helin et al., 2018; Diaz Resquin et al., 2018; Cheng et al., 2022). Consequently, the pair λ_1 = 470 and λ_2 = 950 was adopted in this work for estimating the relative contribution of fossil fuel and biomass burning to the ambient eBC concentration.

The Absorption Ångström Exponents AAE_{ff} and AAE_{bb} represent the spectral dependence of fossil fuel and biomass burning, respectively. Generally, AAE_{ff} and AAE_{bb} are selected from previous experimental results at similar locations or under similar conditions, when auxiliary measurements are not available. Experimental AAE_{ff} values range between 0.9 and 1.1 (Favez et al., 2010; Zotter et al., 2017; Helin et al., 2018; Mousavi et al., 2019).

In this work, the experimental value of AAE_{ff} was determined from b_{abs} at 470 and 950 nm obtained during the weekday morning rush hours (7–9 LT). Previous results in our measurement site have shown that b_{abs} and AAE follow daily patterns according to traffic intensity variability (Segura et al., 2016; Matos et al., 2025). Fig. S1 represents the Ångström matrix (AAE vs. SAE) during weekday morning rush hours (7–9 AM). The BC is the predominant aerosol type (60%), followed by mixtures of large particles and BC (30%). The median AAE obtained from b_{abs} during daily rush period was assumed as our experimental $AAE_{ff} = 1.25 \pm 0.08$.

Our experimental AAE_{ff} value is slightly higher compared to the typical values range (0.9–1.1). The reason is the compensation applied to the b_{abs} from the AE-31 measurements. Assuming a value of C = 2.14, as proposed by Weingartner et al. (2003) (the most commonly used method of compensation in the absence of complementary instrumentation), instead of the experimental compensation, we obtain $AAE_{ff} = 1.04$. However, the site-specific compensation must be applied when the required instrumentation is available, being the Weingartner et al. (2003) proposal only an alternative compensation.

While for diesel/road traffic emissions there is a consensus on the value of the AAE (~1), AAE for biomass burning emissions is not so well-defined. Wood or biomass smoke often contains other organic compounds, such as PAHs or BrC, which absorb mainly in the blue and UV region of the spectrum. This strong absorption at lower wavelengths leads to an increase in AAE (Tiwari et al., 2014). The AAE value in the case of these mixtures depends on several factors, and it is usually within a wider range (1.5–2.2), depending on the type of biomass and combustion efficiency (Favez et al., 2010), the combustion regime (higher the slower the combustion) (Garg et al., 2016) and the state of internal mixing with other non-absorbing components, leading to the large discrepancies in values.

The site-specific value of AAE_{bb} was selected by analyzing different values in the most typical range of experimental values: 1.6–2.2 (Sandradewi et al., 2008a; Diaz Resquin et al., 2018; Mousavi et al., 2019). In this work, a similar procedure applied by Dumka et al. (2019), Jing et al. (2019) and Shen et al. (2021) was used. Basically, the procedure was as follows: (1) assuming the experimental value of AAE_{ff} equal to 1.25, the AM is applied following Eqs. (3)–(6) and varying AAE_{bb} in intervals of 0.2 (from 1.6 to 2.2); (2) the number of negative values of each contribution (eBC_{ff} and eBC_{bb}) was evaluated. The higher the value of AAE_{bb}, the lower the number of negative values of eBC_{ff}; (3) the number of P values (Eq. (6)) less than 0.2 at peak traffic hours (7–9 LT) was calculated, i.e. the number of occurrences the biomass burning contribution was more than 80% being the traffic the dominant contribution. With this criteria, higher values of the AAE_{bb} (1.8–2.2) provide better results; (4) finally, $AAE_{bb} = 2.0$ is chosen and the graphical method was applied (Figure S2), obtaining a value of $AAE_{bb} = 2.11$ (calculating the AAE when P = 0 from the equation of the linear fit). Shen et al. (2021) obtained a similar value (2.16) following the same method, and also the value obtained by Titos et al. (2017) in Granada and by Diapouli et al. (2017) in Athens (2.0) is consistent with that obtained in the present work.

3.3. Convert $b_{abs}(\lambda)$ to eBC concentration

The $b_{abs}(\lambda)$ are converted into equivalent Black Carbon (eBC) concentrations (Petzold et al., 2013) using the Mass Absorption Cross section (MAC):

$$eBC(\lambda) = \frac{b_{abs,\lambda}}{MAC_{\lambda}} \tag{7}$$

Several variables strongly influence the value of the MAC, such as particle size, morphology or mixing state (Zanatta et al., 2016; Zotter et al., 2017), as well as location (Herich et al., 2011; Savadkoohi et al., 2024). Because of the insufficient instrumentation required to determine the MAC experimentally, it is crucial to select a well representative value for our station. In this study, we used a reference MAC value obtained at an urban background site in Barcelona (Spain), by Yus-Díez et al. (2022): 7.55 ± 2.06 m^2 g^{-1} at 950 nm. The principal factor considered in selecting this reference value is the significant local traffic influence at both locations, along with similar atmospheric and geographical conditions.

3.4. Mann–Kendall and Sen's slope estimator

The temporal trends exhibited by the concentrations of eBC_{ff} and eBC_{bb} were analyzed using the Mann–Kendall (MK) test (Mann, 1945; Kendall, 1975). This is one of the most widely used non-parametric tests for estimating trends in aerosol properties, particularly useful when there are missing values, negatives or values below the detection limits in the database. The Sen's slope estimator (Theil, 1950; Sen, 1968), also a non-parametric test, is closely related to MK test, since it determines the magnitude of change. The Sen's slope represents the global slope of the entire time series, and it is calculated as the median of the slopes between each pair of time values.

Kendall (1975) demonstrated that when the number of values in the time series (n) is as small as 10 the normal approximation can be used unless there are numerous tied data (Gilbert, 1987). On the other hand, if data exhibit seasonal changes, they should be considered before applying the MK test. Hirsch et al. (1982) extended the MK test to account for seasonality, resulting in what is known as the seasonal MK test. Essentially, daily medians concentrations are segmented by meteorological seasons, and the procedure is applied using the seasonal or monthly medians, instead of the annual values.

MK test also requires serially uncorrelated time series. There are several methods proposed to eliminate or reduce the autocorrelation, known as "prewhitening". Yue et al. (2002) proposed the *Trend-Free PreWhitening* (TFPW) procedure, compared by Collaud Coen et al. (2020b) with five other prewhitening algorithms, being one of the most common. The daily medians of eBC_{ff} and eBC_{bb} concentrations show a statistically significant autocorrelation, so the algorithm proposed by Yue et al. (2002) was applied before the seasonal MK test. The confidence levels chosen for identifying statistically significant trends in eBC_{ff} and eBC_{bb} concentrations were 80%, 90%, 95% and 99%. The annual trends are considered only if the seasonal slopes are homogeneous at the 90% confidence level (Gilbert, 1987; Collaud Coen et al., 2020a). The seasonal MK test was also applied to eBC_{ff} during rush hours. In addition, the test was applied to daily traffic, in order to compare with eBC_{ff} concentrations trends.

4. Results and discussion

Hourly concentrations of eBC_{ff} and eBC_{bb} were calculated from compensated b_{abs}. The statistics were calculated ensuring the availability of more than 60% of data and removing the measurements corresponding to COVID-19 lockdown period (March 14 to June 15, 2020). The changes exhibited by traffic and total eBC concentrations during this period have been analyzed in Matos et al. (2025).

4.1. Interannual evolution

Fig. 2 shows the evolution of the daily averages of the concentration of both contributions eBC_{ff} and eBC_{bb} from April 2011 to March 2023. The eBC_{bb} concentrations in Fig. 2(b) are much lower than eBC_{ff} concentration in Fig. 2(a): most daily levels are between 0 and 0.2 μg m^{-3}, while the traffic component levels are often ranging between 0.5 and 2 μg m^{-3}.

The annual means (± standard deviation) of eBC_{ff} range from 0.7 ± 0.4 μg m^{-3} to 1.1 ± 0.5 μg m^{-3}, being the average for the entire period 0.9 ± 0.4 μg m^{-3}. The eBC_{ff} levels in other Spanish regions are usually higher; most of them are urban background stations but the measurement periods are usually shorter. Casquero-Vera et al. (2021) obtained in Granada (southern Spain) eBC_{ff} levels of 1.9 ± 2.2 μg m^{-3}

at a suburban station and 2.3 ± 2.6 μg m^{-3} at an urban station, during a winter campaign (December 2015–April 2016). The higher values should also be related to the season. At the same location, Savadkoohi et al. (2023) obtained eBC$_{ff}$ concentration of 1.45 μg m^{-3} during two years (2017–2019). Savadkoohi et al. (2023) also report eBC$_{ff}$ concentrations at two urban background stations: 1.12 μg m^{-3} and 1.26 μg m^{-3} in Madrid and 1.29 μg m^{-3} in Barcelona. eBC$_{ff}$ concentrations at Burjassot are similar to those measured at other traffic stations in Europe (Healy et al., 2017; Savadkoohi et al., 2023), and lower than the results reported by Diaz Resquin et al. (2018) in the Metropolitan Area of Buenos Aires (Argentina), where the medians were in the range 1.23–3.57 μg m^{-3}; or in Nanjing (China), where Shen et al. (2021) found levels of eBC$_{ff}$ between 0.90 ± 0.72 μg m^{-3} and 2.46 ± 1.66 μg m^{-3} during one year.

The interannual evolution of eBC$_{ff}$ is quite similar to total eBC levels (Matos et al., 2025). The reason is the dominance of the traffic contribution, represented by P (Eq. (6)). The mean and median values of P (± standard deviation) for the entire period are 92 ± 11% and 95 ± 11%, respectively, evidencing the traffic as the main source of eBC at the suburban station. Savadkoohi et al. (2023) found similar P values in urban locations in Madrid and Barcelona (Spain) (> 80%), and also in several European locations such as Paris (France) (88%), Hyytiälä (Finland) (89%) and Stockholm (Sweden) (87%). Similar contributions were also found in other European urban stations (Herich et al., 2011; Tiwari et al., 2014; Healy et al., 2017; Zotter et al., 2017; Mousavi et al., 2018; Diaz Resquin et al., 2018; Cheng et al., 2022); and lower than those measured in rural locations where residential wood combustion is more frequent, especially in winter for home heating (Healy et al., 2017; Mbengue et al., 2020), but also in suburban or residential city-areas where wood burning for heating is typically used during the winter (Herich et al., 2011; Healy et al., 2017; Zotter et al., 2017; Helin et al., 2018; Jing et al., 2019; Mbengue et al., 2020; Shen et al., 2021).

In the case of the eBC$_{bb}$ (Fig. 2(b)), the concentrations are clearly lower than eBC$_{ff}$ levels. The annual means range between 0.04 and 0.09 μg m^{-3}. Levels corresponding to 2012 are specially high. According to the Spanish National Inventory of Atmospheric Pollutants (NIAP), which reports emissions of air pollutants, BC emissions due to forest fires increased in 2012, 2015, 2017, 2019 and 2021. The increase of forest fires may be related to some variations in eBC$_{bb}$ concentrations linked to the transport of particles from other regions.

The mean (± standard deviation) of eBC$_{bb}$ over the entire period (2011–2023) is 0.06 ± 0.05 μg m^{-3}, considerably lower than that obtained in the rest of urban background stations in Spain (Becerril-Valle et al., 2017; Casquero-Vera et al., 2021; Savadkoohi et al., 2023) and similar to that obtained by Diaz Resquin et al. (2018) in Metropolitan Area of Buenos Aires (Argentina): 0.06 (0.02–0.13) μg m^{-3}; also in the range of levels obtained at 7 stations near to busy highways (>10k vehicles per day) reported by Healy et al. (2017) in Ontario (Canada): 0.08–0.25 μg m^{-3}; and very close to that determined by Cheng et al. (2022) at a traffic location in Taiwan. The eBC$_{bb}$ concentrations in Burjassot are lower compared to levels where biomass burning is prevalent, such as residential (Helin et al., 2018) or rural areas (Healy et al., 2017).

Fig. 3 shows the interannual evolution of atmospheric variables (temperature, T; relative humidity, RH; wind speed, u; boundary layer height, BLH) and traffic intensity, all of them following a particular annual patterns. The atmospheric variables (Figs. 3(a)–3(d)) indicate that the climatic conditions in Burjassot are characterized by mild winters, with the lowest temperatures rarely falling below 10 °C, and hot, humid summers, with maximum temperatures around 25–30 °C and relative humidity approximately 60%. Additionally, relative humidity, wind speed and boundary layer height exhibit greater variability during the winter months.

Moreover, daily traffic consistently ranges between 100k and 150k vehicles throughout the year, with the exception of August. This annual minimum is attributable to the summer vacation period, which

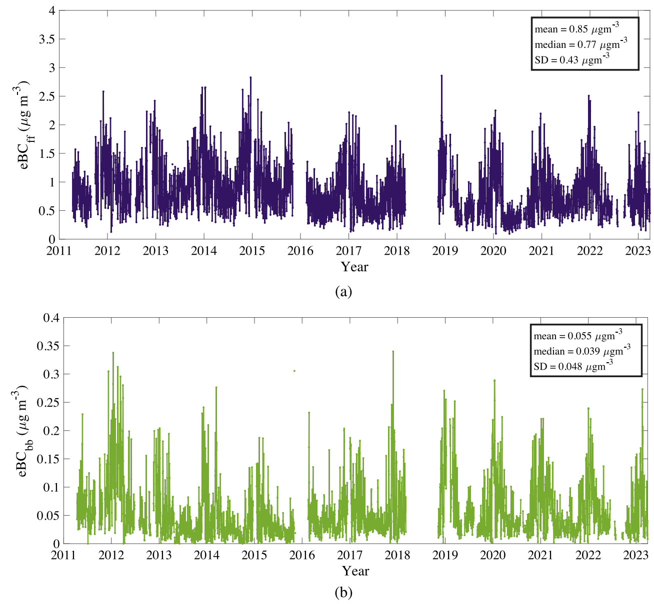

Fig. 2. Interannual evolution of daily means concentrations of (a) eBC$_{ff}$ and (b) eBC$_{bb}$ from April 2011 to March 2023.

results in a significant decrease in daily traffic. Fig. 3(e) also shows a significant reduction of traffic resulting from the lockdown implemented in March 2020 to avoid the spread of the respiratory syndrome coronavirus 2 (SARS-COV-2), responsible for COVID-19. Matos et al. (2025) analyzed the annual variation of traffic on the CV-35 highway during 2020, comparing it with previous and subsequent years. The 60% decrease in daily traffic was unequivocally related to the 50% lower concentration of total eBC at our measurement site. In this study, contributions from traffic and biomass burning during the confinement period exhibited reductions of 53% and 14%, respectively.

4.2. Intra-annual evolution

The intra-annual characterization of V, BLH and both eBC components concentrations is shown in Fig. 4, where the monthly distribution based on daily concentrations is represented using box-whiskers plots. The horizontal line in each box is the median (50th percentile), edges of each box are the 25th and 75th percentiles, being the distance between the two extremes the interquartile range. The whiskers indicate the 5th and 95th percentiles. Data exceeding the whisker length are marked as outliers. The asterisk in each box is the mean value.

Daily eBC$_{ff}$ and eBC$_{bb}$ concentrations in Burjassot show a marked annual pattern, with higher values in winter, while the lower levels occur in summer. This seasonality seems mainly due to atmospheric influence: both atmospheric variables (u and BLH) show a particular seasonal pattern. The daily development of the Atmospheric Boundary Layer (ABL) depends directly on the temperature, which also has a strong seasonal character (Fig. 3(a)). The lower the temperature, the more limited the vertical development of the ABL. Higher concentrations of eBC$_{ff}$ and eBC$_{bb}$ in winter are due to a combined effect of lower BLH and frequent stagnation events.

In addition, Fig. 4 confirms the variability in winter months, showing by larger interquartile range. The variability of daily concentration in winter and autumn is related to the greater variability also observed in atmospheric conditions (Figs. 4(a) and 4(b)). The annual medians are slightly lower than the averages, which usually occurs in long-term temporal series, due to the high temporal variability and outliers occurrences.

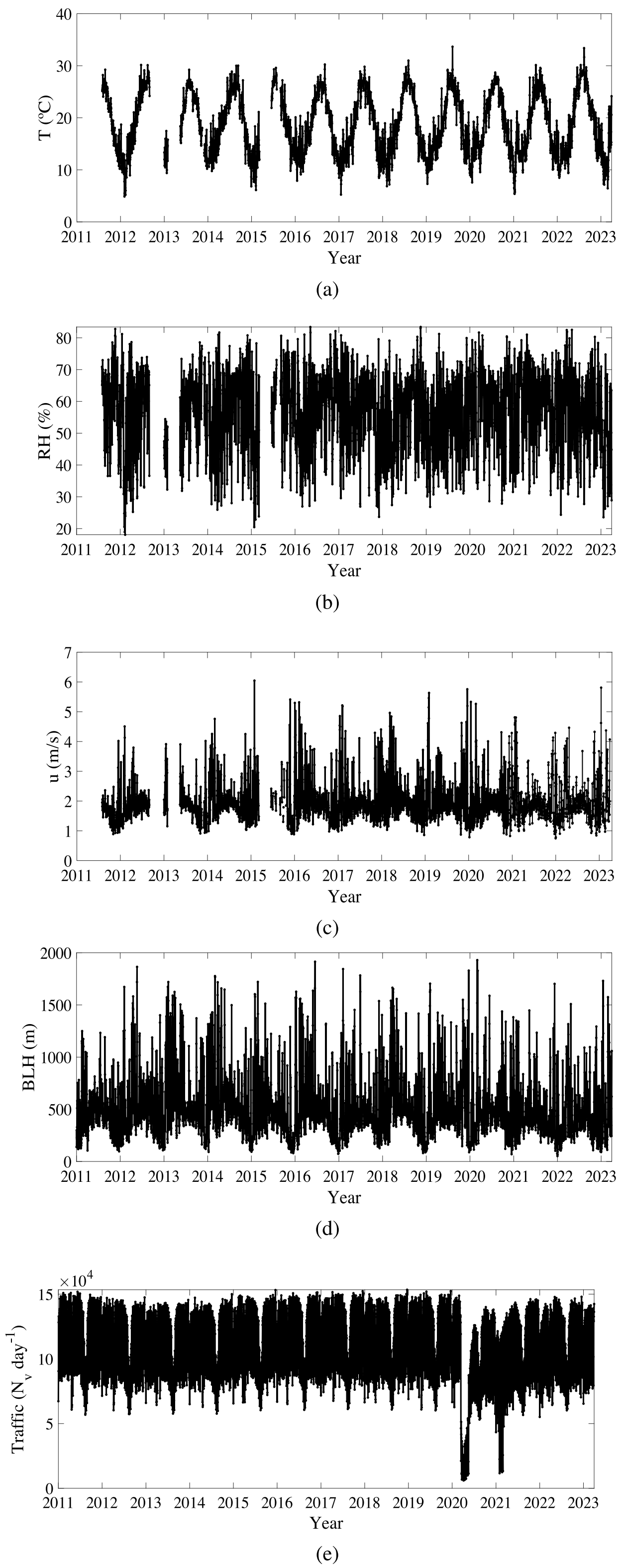

Fig. 3. Interannual evolution of daily (a) temperature (T), (b) relative humidity (RH), (c) wind speed (u), (d) boundary layer height (BLH) and (e) traffic intensity.

The daily traffic intensity on the highway near our measurement site does not exhibit clear seasonality (Matos et al., 2025). Consequently, the seasonality observed in the eBC_{ff} and eBC_{bb} concentrations does not appear to correlate with seasonal variations in local traffic.

Table 1
Seasonal MK test statistics of eBC_{ff} and eBC_{bb} at Burjassot station: number of seasonal data (N), test statistic (Z), Sen's slope (Sen), Confidence Intervals of the slope at 90% confidence level (CI), interpretation of the trend (Trend): ↑ (increasing), ↓ (decreasing) and ⊗ (no trend); and significance level of the test (Sign): α= 0.01(****), 0.05(***), 0.1(**) and 0.2(*).

	N	Z	Sen μg m^{-3}/yr (%/yr)	CI μg m^{-3}	Trend	Sign
eBC_{ff}						
Winter	12	−2.40	−0.017 (−6.6)	(−0.026, −0.006)	↓	***
Spring	13	−2.87	−0.018 (−10.7)	(−0.024, −0.009)	↓	****
Summer	11	−3.89	−0.024 (−16.6)	(−0.028, −0.018)	↓	****
Autumn	12	−3.91	−0.033 (−15.4)	(−0.036, −0.028)	↓	****
Annual	48	−6.59	−0.023 (−12.4)	(−0.026, −0.019)	↓	****
eBC_{bb}						
Winter	12	1.71	0.0016 (8.3)	(0.0002, 0.0031)	↑	**
Spring	13	0.67	–	–	⊗	–
Summer	11	2.96	0.0009 (8.7)	(0.0006, 0.0015)	↑	****
Autumn	12	1.57	0.0011 (9.7)	(−0.0003, 0.0022)	↑	*
Annual	48	3.44	–	–	⊗	–

4.3. Annual and seasonal trends

Over the last years, various aerosol optical and radiative properties have been suffered reductions across Europe, particularly in urban sites highly influenced by traffic (Sun et al., 2020; Luoma et al., 2021; Savadkoohi et al., 2023). These trends highlight the effectiveness of the regulations implemented for reducing anthropogenic emissions and improving air quality. This section focuses on the assessment of the temporal trends exhibited by the eBC_{ff} and eBC_{bb} concentrations. The seasonal MK test and Sen's slope estimator were applied, with slopes normalized to facilitate the interpretation of the trends

Table 1 presents the test statistics exhibited by seasonal concentrations of both components. The eBC_{ff} concentration shows statistically significant (ss) decreasing trends in all seasons, at higher than 90% confidence level, which allows to determine the annual decreasing trend of the traffic contribution, and the slope is −12.4%/yr at 99% confidence level. The inter-annual reduction of eBC_{ff} is consistent with data reported in the NIAP: annual estimates of emissions of the primary atmospheric pollutants (NO_x, PM and BC) are reported for the period 1900–2021. Emissions of NO_x from road transport decreased by 50.7% since 1990 and 52.7% since 2011. National BC emissions due to on-road traffic have decreased by 42% since 2011. These trends are consistent with the findings of Sun et al. (2020), who observed decreasing eBC concentrations from 2009 to 2018 at 16 stations in Germany with a 95% confidence level. Similar trends of eBC_{ff} have been reported in other urban sites, primarily in Europe. The trends of eBC_{ff} also agree with the decreasing trends observed in total eBC at our measurement site by Matos et al. (2025). The seasonal concentrations of total eBC decreased annually since 2011, with slopes varying from −15%/yr (autumn) to −5.0%/yr (winter). Matos et al. (2025) also studied the temporal trends of the AAE, showing increasing trends for all seasons at 99% confidence level. Aerosol properties such as AOD (Aerosol Optical Depth) and b_{abs} have exhibited decreasing trends in recent years (Collaud Coen et al., 2020a; Gupta et al., 2022). At our measurement site, Garcia-Suñer et al. (2023) found statistically significant (at > 80% confidence level) decreasing trend in AOD for most months; whereas AE and SSA do not show statistically significant long-term trends, only for a few months of the year.

On the contrary, not ss annual trend was found for eBC_{bb} concentrations. In this case, seasonal MK test determined ss increasing trends in winter, summer and autumn, with slopes ranging 8–10%/yr, at 90%, 99% and 80% confidence levels, respectively. Similar trends have been observed in several European locations, related to the increase in biomass burning for domestic and commercial uses (Mousavi et al., 2018; Savadkoohi et al., 2023).

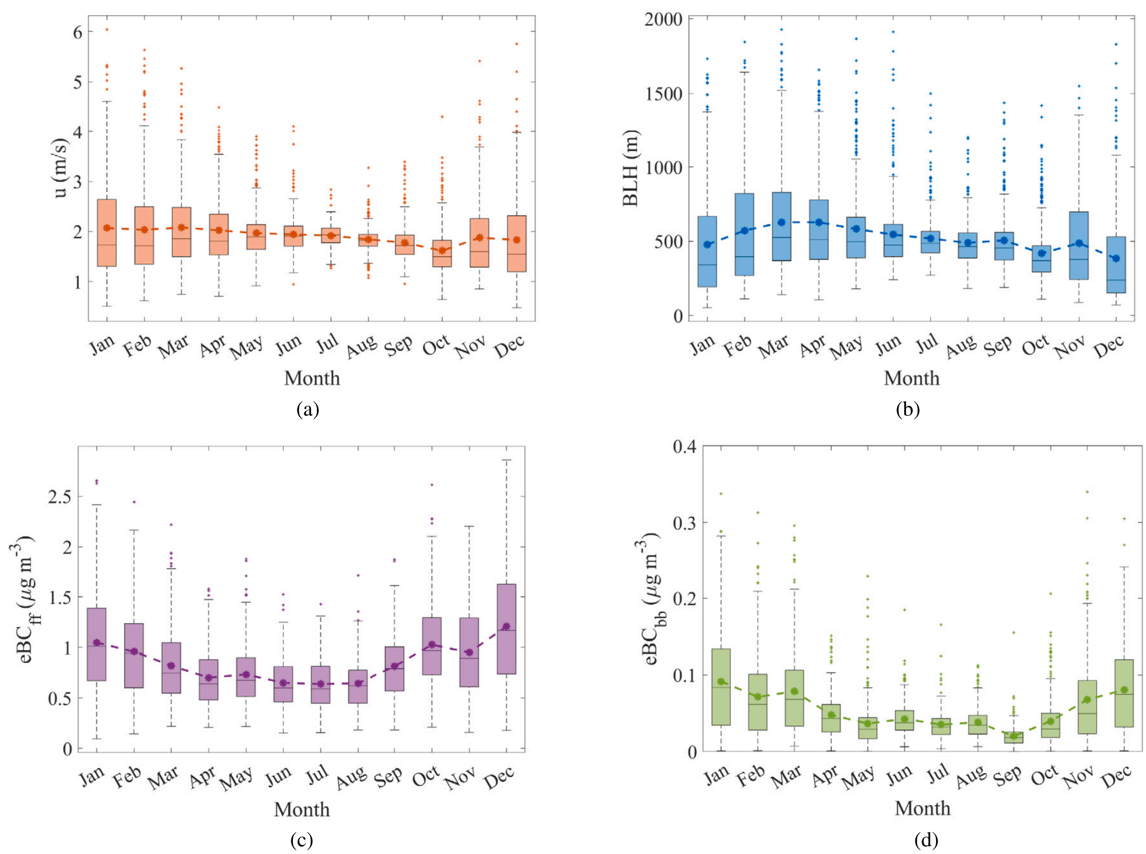

Fig. 4. Monthly box-whisker distribution (based on daily means) of (a) wind speed (V), (b) Boundary Layer Height (BLH), (c) eBC$_{ff}$ and (d) eBC$_{bb}$ concentrations. Confinement period (March 15-June 22, 2020) was removed in c and d.

The traffic influence on eBC$_{ff}$ concentrations requires an in-depth study of the temporal variations of traffic in the metropolitan area of Valencia, which allows relating the eBC$_{ff}$ concentrations trends to the traffic as the main emission source. For this purpose, the seasonal MK test was applied to the daily traffic intensity. The only "seasonal" dependence of traffic is the annual minimum reached in August (Fig. 3(e)). For the rest of the year, daily traffic is relatively constant. To respect its seasonality, the MK test is applied to daily light, heavy and total traffic for all months excluding August, and for August data separately. A distinction was also made between traffic on WeekDays (WD) and WeekEnd days (WE), as the daily traffic pattern changes during the week. Statistics values of seasonal MK test are presented in Table 2.

Generally, eBC$_{ff}$ concentrations showed a decreasing trend over the years, but traffic does not show the same behavior. As shown in Table 2, light traffic shows decreasing trends for weekdays and weekends, but they are ss only for weekends at 99% confidence level, with a very low slope (-0.1%/yr). On the other hand, heavy traffic shows more temporal trends, although they are not homogeneous. For weekdays, increasing trend is found, with a slope of 1.4%/yr in August; while on weekends a decreasing trend is exhibited (at 90% confidence level) only for monthly values excluding August. The trends found in total traffic are similar to those of light traffic, since it is predominant.

Following the results of Table 2, there is no direct relationship between the trends of traffic and eBC$_{ff}$ concentrations. The temporal decrease in traffic is not the only factor to consider when analyzing pollutant trends. While traffic may remain constant over time, emissions may suffer changes, primarily related to air pollution controls and new emission standards, as well as the recent increase of electric and hybrid vehicles (both in public and particular transport). This may be related to the reduction of the levels of primary pollutants, such as BC, even if the traffic intensity is constant or increasing (Järvi et al., 2008; Luoma et al., 2021).

4.4. *Diurnal variability*

The daily variability of eBC$_{ff}$ and eBC$_{bb}$ is presented in Fig. 5, where seasonally (winter, spring, summer and autumn) and weekly (weekdays and weekends) separation was made, in order to analyze the *weekend effect* on the concentrations, as well as the seasonal dependence of atmospheric variables.

The daily pattern shown by eBC$_{ff}$ is the typical shape reported in locations strongly influenced by traffic (Herich et al., 2011; Tiwari et al., 2014; Helin et al., 2018; Jing et al., 2019; Shen et al., 2021; Luoma et al., 2021). Basically, the pattern is characterized by a first morning peak (between 7–9 LT) and a second peak in the evening (between 19–21 LT). The second peak almost disappears in spring and summer, which is usually related to a combination of higher atmospheric turbulence conditions with higher BLH. The disappearance of the second peak of eBC$_{ff}$ in spring and summer is also related to the reduction in traffic during the summer due to the adjustment of working hours, with earlier departures from work. These peaks, mainly observed on weekdays, are clearly related to the traffic daily maximum occurring between 7–9 LT and 18–20 LT for both light and heavy vehicles on weekdays (Fig. 6). The *weekend effect* is evident in Fig. 5(a–d), where the morning peak is markedly reduced, showing another afternoon peak, especially in winter and autumn. This second daily peak is related to the increase in traffic in the evening on weekends (Fig. 6). Generally, eBC$_{ff}$ levels on weekends are lower and show a smoother pattern than weekdays levels, due to decreases of 70% and 30% in heavy and light traffic, respectively. However, at earlier hours of the weekend days, eBC$_{ff}$ concentrations are highest, because the

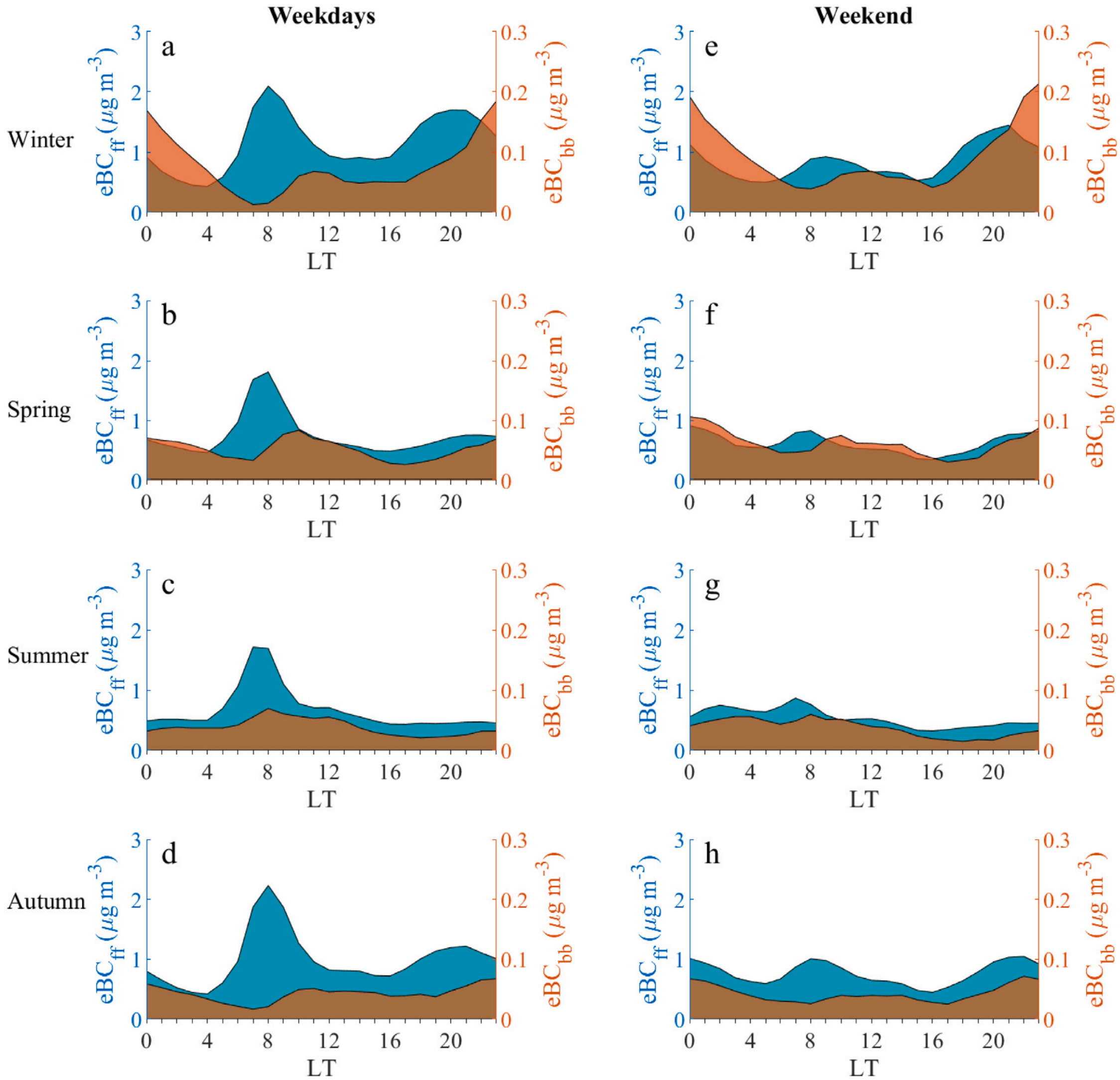

Fig. 5. Daily-seasonal variability of eBC_{ff} and eBC_{bb} concentrations on (a–d) weekdays and (e–h) weekends.

nighttime traffic intensity is higher than on weekdays (Fig. 6(a)). The minimum eBC_{ff} concentrations at noon is related to the maximum daily BLH and wind speed (Matos et al., 2025), favoring pollutant dispersion and causing concentrations to decrease.

Levels of eBC_{bb} do not show significant changes during the week, which is also common in traffic influenced locations (Zotter et al., 2017; Becerril-Valle et al., 2017). However, slightly higher concentrations are reached on weekends, mainly in winter, which may be related to the transport of some nearby contribution. On weekends, travels by car to rural areas are typical, being likely that the higher eBC_{bb} concentrations in winter may be due to emissions from wood burning for heating from towns around Valencia.

Therefore, changes observed in eBC components concentrations during the day are mainly governed by traffic (especially on weekdays for eBC_{ff}) and atmospheric variables (BLH and wind speed).

4.4.1. Maximum eBC_{ff} concentrations trends

As discussed in Section 4.3, daily traffic does not exhibit ss trends. However, the eBC_{ff} concentrations do exhibit ss decreasing trends for all seasons. Considering the relevance of traffic in the measurements, seasonal MK test was applied to concentrations during rush hours, when the traffic influence is stronger, in order to analyze the temporal trends of temporally segregated eBC_{ff} concentrations.

Table 3 shows the MK statistics corresponding to eBC_{ff} concentrations around the first morning traffic peak (TR1), between 7–9 LT, and the second evening traffic peak (TR2), which occurs at 20 LT. The eBC_{ff} concentrations exhibit ss decreasing trends in all seasons, at 90% (or higher) confidence levels. The annual slopes varies between −5%/yr and −2.6%/yr for the morning peak and −5.5%/yr and −3.1%/yr for the second peak. There are also seasonal differences in the trends. For example, the relative annual decrease is higher in autumn and summer comparing with winter trends, which is also observed in Table 1. In addition, the confidence level is also lower in winter. Although the exhibited changes of eBC_{ff} concentration may have a direct dependence on the temporal variability of traffic emissions, the seasonal differences may be due to the fact that traffic in winter is not the main influence on eBC_{ff} changes. Due to the atmospheric conditions during winter (mainly atmospheric instability), the observed changes in eBC_{ff} concentrations may be more influenced by atmospheric conditions than by traffic. Therefore, the decrease in eBC_{ff} during winter is less significant, as it depends on atmospheric conditions, which have not changed interannually at our location (Matos et al., 2025).

The seasonal MK test was also applied to traffic intensity during rush hours (TR1 and TR2) and not ss trends were found. Therefore, decreasing trends exhibited by eBC_{ff} concentrations are more related to changes in traffic emissions rather than traffic intensity.

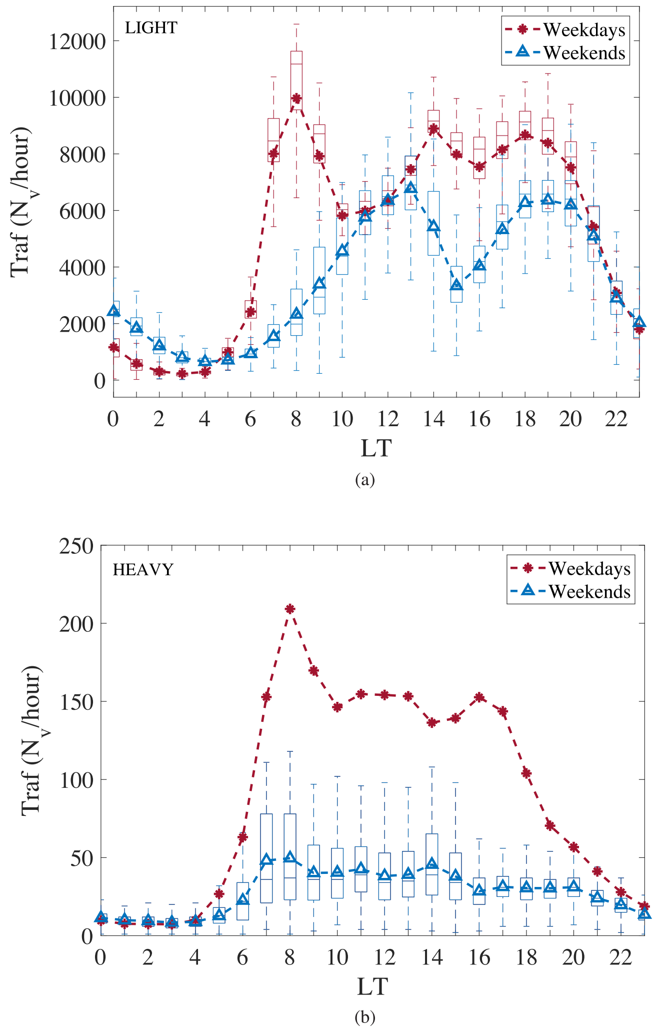

Fig. 6. Daily variability of (a) light (a) and (b) heavy traffic on weekdays (red) and weekends (blue).

Table 2
Seasonal MK statistics of daily traffic intensity: test statistic (Z), Sen's slope (Sen), Confidence Intervals of the slope at 90% confidence level (CI), interpretation of the trend (Trend): ↑ (increasing), ↓ (decreasing) and ⊗ (no trend); and significance level of the test (Sign): α= 0.01(****), 0.05(***), 0.1(**) and 0.2(*).

Period[a]	Z	Sen (N_c/day)/yr (%/yr)	CI (N_c/yr)	Tend	Sign
Light					
Mensual-WD	−1.17	–	–	⊗	–
Aug-WD	0.48	–	–	⊗	–
Mensual-WE	−3.83	−61 (−0.1)	(−86.98, −34.26)	↓	****
Aug-WE	0.34	–	–	⊗	–
Heavy					
Mensual-WD	1.39	0.53 (0.02)	(−0.13, 1.15)	↑	*
Aug-WD	1.71	22.05 (1.42)	(4.89, 36.20)	↑	**
Mensual-WE	−1.75	−0.44 (−0.06)	(−0.90, −0.02)	↓	**
Aug-WE	−1.03	–	–	⊗	–
Total					
Mensual-WD	−1.18	–	–	⊗	–
Aug-WD	0.34	–	–	⊗	–
Mensual-WE	−3.82	−61.63 (−0.07%)	(−34.58, −0.07)	↓	****
Aug-WE	0.34	–	–	⊗	–

[a] Periods: *Mensual* (all months excluding August); *WD* (WeekDays); *WE* (WeekEnds).

Table 3
Seasonal MK test statistics of eBC_{ff} during traffic peaks: number of seasonal data (N), test statistic (Z), Sen's slope (Sen), Confidence Intervals of the slope at 90% confidence level (CI), interpretation of the trend (Trend): ↑ (increasing), ↓ (decreasing) and ⊗ (no trend); and significance level of the test (Sign): α= 0.01(****), 0.05(***), 0.1(**) and 0.2(*).

Period[a]	N	Z	Sen μg m^{-3}/yr (%/yr)	CI μg m^{-3}	Tend	Sign
eBC_{ff}						
Winter-TR1	12	−1.44	−0.045 (−2.6)	(−0.090,0.001)	↓	*
Spring -TR1	13	−2.26	−0.048 (−2.9)	(−0.083, −0.019)	↓	***
Summer-TR1	11	−2.49	−0.085 (−5.0)	(−0.119, −0.065)	↓	***
Autumn-TR1	12	−2.26	−0.101 (−5.0)	(−0.155, −0.022)	↓	***
Annual-TR1	48	−4.33	–	–	⊗	–
Winter-TR2	12	−1.58	−0.057 (−4.3)	(−0.102, 0.002)	↓	*
Spring-TR2	13	−1.89	−0.017 (−3.1)	(−0.040, −0.004)	↓	**
Summer-TR2	11	−2.18	−0.021 (−5.3)	(−0.030, −0.010)	↓	***
Autumn-TR2	12	−2.67	−0.062 (−5.5)	(−0.085, −0.028)	↓	****
Annual-TR2	48	−4.26	–	–	⊗	–

[a] Traffic peaks: TR1 (7-9 LT) and TR2 (18-21 LT).

5. Main conclusions

This work is the first climatological study on traffic and biomass burning contributions to equivalent Black Carbon carried out in Valencia. During 12 years, fossil fuel (eBC_{ff}) and biomass burning (eBC_{bb}) contributions were estimated using a source apportionment method (Aethalometer Model). The temporal analysis includes four time scales: interannual, intra-annual, daily and seasonal, but also the relation between both contributions of eBC with atmospheric and anthropogenic variables. The second general objective of this work was to determine the existence of decreasing/increasing trends of the eBC_{ff} and eBC_{bb} concentrations, applying the non-parametric seasonal Mann–Kendall test and Sen's slope estimator. The main conclusions of this work are:

The average daily concentration (± standard deviation) between 2011 and 2023 of eBC_{ff} was 0.9 ± 0.5 μg m^{-3}, while the mean daily concentration of eBC_{bb} was 0.06 ± 0.05 μg m^{-3}. The difference between the two contributions is the evidence of the anthropogenic character of the local absorbing aerosols. The average value of P (eBC_{ff}/eBC) over the entire study period is 92 ± 11%, demonstrating the strong influence of traffic emissions on the measurements.

The concentrations of eBC_{ff} and eBC_{bb} showed a marked seasonal dependence, characterized by higher values in winter than in summer. The annual changes are related to the annual evolution of the boundary layer height, but also to the seasonality of wind speed. Both variables reach their higher values in summer, facilitating the dispersion of the pollutants.

Concentrations of eBC_{ff} also show a daily variability: one morning peak around 7–8 LT and other second peak around 20 LT (in autumn and winter). This behavior corresponds with typical increase of traffic intensity in the early morning and late afternoon (rush hours). During weekends, these peaks are considerably reduced, which is consistent with the decrease in traffic. The minimum concentration observed at noon is related to the maximum boundary layer height, and not due to the traffic, since it increases at 14 LT. On the contrary, the concentrations of eBC_{bb} does not have a marked daily variability. The concentration during winter days seems to be higher at night than during the day. Since there appear to be no local sources of emission, the concentration of eBC_{bb} is expected to be more related to the atmospheric boundary layer, which is developing during the day as the temperature increases. This causes pollutants that were confined in the stable boundary layer (or nighttime boundary layer) to disperse, reducing the surface concentration.

The eBC_{ff} concentrations show statistically significant decreasing trends in all seasons. The Sen's slopes are −16.6%/yr in summer, −15.4%/yr in autumn, −10.7%/yr in spring and −6.6%/yr in winter at 99%, 99%, 99% and 95% confidence levels, respectively. The annual slope of eBC_{ff} is −0.023 μg m^{-3}/yr or −12.4%/yr. Applying the seasonal MK test to the concentrations of eBC_{ff} during the two daily peaks of traffic, statistically significant decreasing trends are also found for all seasons. These results provide clear conclusions: the concentrations of eBC associated with traffic emissions has been significantly reduced since 2011. However, traffic intensity does not show statistically significant trends to explain the reduction observed in concentrations. The decreasing trends exhibited by eBC_{ff} are related to reductions or changes in local traffic emissions.

On the contrary, eBC_{bb} concentrations exhibit increasing trends in all seasons except to spring time. The slopes of the trends are 8.3%/yr in winter, at 90% confidence level; 8.7%/yr in summer, at 99% confidence level; and 9.7%/yr in autumn at 80% confidence level. Biomass burning of anthropogenic origin is related to heating installations and regional agricultural fires, so the positive slopes may be related to the increase in biomass burning installations in the rural surroundings of Valencia.

Based on these conclusions, future research directions may focus on quantifying the influence of several factors (both atmospheric and anthropogenic) on the contributions of traffic and biomass burning to ambient eBC. The findings of this study offer essential insights for the development of policies aimed at regulating anthropogenic emissions. Consequently, it is vital to continue monitoring the concentration of eBC in metropolitan areas, where traffic plays a predominant role.

CRediT authorship contribution statement

Violeta Matos: Writing – review & editing, Writing – original draft, Visualization, Validation, Software, Methodology, Investigation, Formal analysis, Conceptualization. **Mar Sorribas:** Writing – review & editing, Validation, Supervision, Resources, Methodology, Investigation, Formal analysis, Conceptualization. **Sara Segura:** Software, Resources, Methodology, Data curation. **María Pilar Utrillas:** Writing – review & editing, Supervision, Project administration, Funding acquisition. **Víctor Estellés:** Writing – review & editing, Visualization, Validation, Supervision, Software, Resources, Project administration, Methodology, Investigation, Funding acquisition, Formal analysis, Data curation.

Declaration of competing interest

The authors declare that they have no known competing financial interests or personal relationships that could have appeared to influence the work reported in this paper.

Acknowledgments

This work was supported jointly by the Science and Innovation Ministry, the State Research Agency and the European Regional Development Fund through projects PID2022-138730OB-I00, PID2021-123881OB-I00, TED2021-129185BI00 and PRE2018-084799; and by the Valencia Autonomous Government (Conselleria d' Educació, Cultura, Universitats i Ocupació) for the projects CIAICO2023-088 and AICO/2021/341.1. We would like to acknowledge the local administration (Direcció General d' Obres Públiques, Transport i Mobilitat Sostenible de la Generalitat Valenciana) for the traffic data provided.

Appendix A. Supplementary data

Supplementary material related to this article can be found online at https://doi.org/10.1016/j.apr.2025.102527.

References

Arnott, W.P., Hamasha, K., Moosmüller, H., Sheridan, P.J., Ogren, J.A., 2005. Towards aerosol light-absorption measurements with a 7-wavelength aethalometer: Evaluation with a photoacoustic instrument and 3-wavelength nephelometer. Aerosol Sci. Technol. 39 (1), 17–29. http://dx.doi.org/10.1080/027868290901972.

Becerril-Valle, M., Coz, E., Prévôt, A., Močnik, G., Pandis, S., Sánchez de la Campa, A., Alastuey, A., Díaz, E., Pérez, R., Artíñano, B., 2017. Characterization of atmospheric black carbon and co-pollutants in urban and rural areas of Spain. Atmos. Environ. 169, 36–53. http://dx.doi.org/10.1016/j.atmosenv.2017.09.014, URL: https://www.sciencedirect.com/science/article/pii/S1352231017306052.

Bond, T.C., Doherty, S.J., Fahey, D.W., Forster, P.M., Berntsen, T., DeAngelo, B.J., Flanner, M.G., Ghan, S., Kärcher, B., Koch, D., Kinne, S., Kondo, Y., Quinn, P.K., Sarofim, M.C., Schultz, M.G., Schulz, M., Venkataraman, C., Zhang, H., Zhang, S., Bellouin, N., Guttikunda, S.K., Hopke, P.K., Jacobson, M.Z., Kaiser, J.W., Klimont, Z., Lohmann, U., Schwarz, J.P., Shindell, D., Storelvmo, T., Warren, S.G., Zender, C.S., 2013. Bounding the role of black carbon in the climate system: A scientific assessment. J. Geophys. Res.: Atmos. 118 (11), 5380–5552. http://dx.doi.org/10.1002/jgrd.50171.

Brewer, T.L., 2020. Black carbon and other air pollutants in Italian ports and coastal areas: Problems, solutions and implications for policies. Appl. Sci. 10 (23), http://dx.doi.org/10.3390/app10238544.

Casquero-Vera, J., Lyamani, H., Titos, G., Minguillón, M., Dada, L., Alastuey, A., Querol, X., Petäjä, T., Olmo, F., Alados-Arboledas, L., 2021. Quantifying traffic, biomass burning and secondary source contributions to atmospheric particle number concentrations at urban and suburban sites. Sci. Total Environ. 768, 145282. http://dx.doi.org/10.1016/j.scitotenv.2021.145282, URL: https://www.sciencedirect.com/science/article/pii/S004896972100348X.

Cheng, Y.-H., Huang, Y.-C., Pipal, A.S., Jian, M.-Y., Liu, Z.-S., 2022. Source apportionment of black carbon using light absorption measurement and impact of biomass burning smoke on air quality over rural central Taiwan: A yearlong study. Atmos. Pollut. Res. 13 (1), 101264. http://dx.doi.org/10.1016/j.apr.2021.101264, URL: https://www.sciencedirect.com/science/article/pii/S1309104221003263.

Collaud Coen, M., Andrews, E., Alastuey, A., Arsov, T.P., Backman, J., Brem, B.T., Bukowiecki, N., Couret, C., Eleftheriadis, K., Flentje, H., Fiebig, M., Gysel-Beer, M., Hand, J.L., Hoffer, A., Hooda, R., Hueglin, C., Joubert, W., Keywood, M., Kim, J.E., Kim, S.-W., Labuschagne, C., Lin, N.-H., Lin, Y., Lund Myhre, C., Luoma, K., Lyamani, H., Marinoni, A., Mayol-Bracero, O.L., Mihalopoulos, N., Pandolfi, M., Prats, N., Prenni, A.J., Putaud, J.-P., Ries, L., Reisen, F., Sellegri, K., Sharma, S., Sheridan, P., Sherman, J.P., Sun, J., Titos, G., Torres, E., Tuch, T., Weller, R., Wiedensohler, A., Zieger, P., Laj, P., 2020a. Multidecadal trend analysis of in situ aerosol radiative properties around the world. Atmos. Chem. Phys. 20 (14), 8867–8908. http://dx.doi.org/10.5194/acp-20-8867-2020.

Collaud Coen, M., Andrews, E., Bigi, A., Martucci, G., Romanens, G., Vogt, F.P.A., Vuilleumier, L., 2020b. Effects of the prewhitening method, the time granularity, and the time segmentation on the Mann–Kendall trend detection and the associated Sen's slope. Atmos. Meas. Tech. 13 (12), 6945–6964. http://dx.doi.org/10.5194/amt-13-6945-2020.

Collaud Coen, M., Weingartner, E., Apituley, A., Ceburnis, D., Fierz-Schmidhauser, R., Flentje, H., Henzing, J.S., Jennings, S.G., Moerman, M., Petzold, A., Schmid, O., Baltensperger, U., 2010. Minimizing light absorption measurement artifacts of the Aethalometer: evaluation of five correction algorithms. Atmos. Meas. Tech. 3 (2), 457–474. http://dx.doi.org/10.5194/amt-3-457-2010, URL: https://amt.copernicus.org/articles/3/457/2010/.

Council of the European Union, 2023. Proposal for a Directive of the European Parliament and of the Council On Ambient Air Quality and Cleaner Air for Europe (Recast), Mandate for Negotiations with the European Parliament. Brussels.

Diapouli, E., Kalogridis, A.-C., Markantonaki, C., Vratolis, S., Fetfatzis, P., Colombi, C., Eleftheriadis, K., 2017. Annual variability of black carbon concentrations originating from biomass and fossil fuel combustion for the Suburban Aerosol in Athens, Greece. Atmos. 8 (12), http://dx.doi.org/10.3390/atmos8120234.

Diaz Resquin, M., Santágata, D., Gallardo, L., Gómez, D., Rössler, C., Dawidowski, L., 2018. Local and remote black carbon sources in the metropolitan area of Buenos aires. Atmos. Environ. 182, 105–114. http://dx.doi.org/10.1016/j.atmosenv.2018.03.018, URL: https://www.sciencedirect.com/science/article/pii/S1352231018301560.

Ding, A.J., Huang, X., Nie, W., Sun, J.N., Kerminen, V.-M., Petäjä, T., Su, H., Cheng, Y.F., Yang, X.-Q., Wang, M.H., Chi, X.G., Wang, J.P., Virkkula, A., Guo, W.D., Yuan, J., Wang, S.Y., Zhang, R.J., Wu, Y.F., Song, Y., Zhu, T., Zilitinkevich, S., Kulmala, M., Fu, C.B., 2016. Enhanced haze pollution by black carbon in megacities in China. Geophys. Res. Lett. 43 (6), 2873–2879. http://dx.doi.org/10.1002/2016GL067745, URL: https://agupubs.onlinelibrary.wiley.com/doi/abs/10.1002/2016GL067745.

Dumka, U., Kaskaoutis, D., Devara, P., Kumar, R., Kumar, S., Tiwari, S., Gerasopoulos, E., Mihalopoulos, N., 2019. Year-long variability of the fossil fuel and wood burning black carbon components at a rural site in southern Delhi outskirts. Atmos. Res. 216, 11–25. http://dx.doi.org/10.1016/j.atmosres.2018.09.016, URL: https://www.sciencedirect.com/science/article/pii/S0169809518307828.

Estellés, V., Martínez-Lozano, J.A., Utrillas, M.P., Campanelli, M., 2007. Columnar aerosol properties in Valencia (Spain) by ground-based sun photometry. J. Geophys. Res.: Atmos. 112 (D11), http://dx.doi.org/10.1029/2006JD008167, arXiv:https://agupubs.onlinelibrary.wiley.com/doi/pdf/10.1029/2006JD008167, URL: https://agupubs.onlinelibrary.wiley.com/doi/abs/10.1029/2006JD008167.

Estellés, V., Utrillas, M.P., Martínez-Lozano, J.A., 2005. Study of a pollution episode in valencia (Spain) due to biomass fires in 'la albufera' rice paddies. In: Proceedings of the 5th International Conference on Urban Air Quality.

Esteve, A.R., Estellés, V., Segura, S., Utrillas, M., Martínez-Lozano, J.A., 2012a. Influence of the trajectory of air masses on the in situ measurements of aerosol properties in Valencia. Tethys J. Weather. Clim. West. Mediterr. 9, 35–41. http://dx.doi.org/10.3369/tethys.2012.9.04.

Esteve, A.R., Estellés, V., Utrillas, M.P., Martínez-Lozano, J.A., 2012b. In-situ integrating nephelometer measurements of the scattering properties of atmospheric aerosols at an urban coastal site in western Mediterranean. Atmos. Environ. 47, 43–50. http://dx.doi.org/10.1016/j.atmosenv.2011.11.043, URL: https://www.sciencedirect.com/science/article/pii/S1352231011012295.

Farzad, K., Khorsandi, B., Khorsandi, M., Bouamra, O., Maknoon, R., 2020. A study of cardiorespiratory related mortality as a result of exposure to black carbon. Sci. Total Environ. 725, 138422. http://dx.doi.org/10.1016/j.scitotenv.2020.138422.

Favez, O., El Haddad, I., Piot, C., Boréave, A., Abidi, E., Marchand, N., Jaffrezo, J.-L., Besombes, J.-L., Personnaz, M.-B., Sciare, J., Wortham, H., George, C., D'Anna, B., 2010. Inter-comparison of source apportionment models for the estimation of wood burning aerosols during wintertime in an alpine city (Grenoble, France). Atmos. Chem. Phys. 10 (12), 5295–5314. http://dx.doi.org/10.5194/acp-10-5295-2010, URL: https://acp.copernicus.org/articles/10/5295/2010/.

Garcia-Suñer, M., Matos, V., Kumar, G., Estellés, V., Utrillas, M., 2023. 20 years of columnar aerosol properties at valencia area (eastern Spain) by ground-based sun-photometry. Atmos. Res. 1, 1.

Garg, S., Chandra, B.P., Sinha, V., Sarda-Esteve, R., Gros, V., Sinha, B., 2016. Limitation of the use of the absorption angstrom exponent for source apportionment of equivalent black carbon: a case study from the North west indo-gangetic plain. Environ. Sci. Technol. 50 (2), 814—824. http://dx.doi.org/10.1021/acs.est.5b03868.

Gilbert, R.O., 1987. Statistical Methods for Environmental Pollution Monitoring. Wiley, New York, USA, p. 336.

Gómez-Amo, J., Estellés, V., Marcos, C., Segura, S., Esteve, A., Pedrós, R., Utrillas, M., Martínez-Lozano, J., 2017. Impact of dust and smoke mixing on column-integrated aerosol properties from observations during a severe wildfire episode over Valencia (Spain). Sci. Total Environ. 599–600, 2121–2134. http://dx.doi.org/10.1016/j.scitotenv.2017.05.041.

Grahame, T.J., Klemm, R., Schlesinger, R.B., 2014. Public health and components of particulate matter: The changing assessment of black carbon. J. Air Waste Manage. Assoc. 64 (6), 620–660. http://dx.doi.org/10.1080/10962247.2014.912692.

Gupta, G., Venkat Ratnam, M., Madhavan, B., Narayanamurthy, C., 2022. Long-term trends in aerosol optical depth obtained across the globe using multi-satellite measurements. Atmos. Environ. 273, 118953. http://dx.doi.org/10.1016/j.atmosenv.2022.118953, URL: https://www.sciencedirect.com/science/article/pii/S1352231022000188.

Healy, R., Sofowote, U., Su, Y., Debosz, J., Noble, M., Jeong, C.-H., Wang, J., Hilker, N., Evans, G., Doerksen, G., Jones, K., Munoz, A., 2017. Ambient measurements and source apportionment of fossil fuel and biomass burning black carbon in ontario. Atmos. Environ. 161, 34–47. http://dx.doi.org/10.1016/j.atmosenv.2017.04.034, URL: https://www.sciencedirect.com/science/article/pii/S1352231017302789.

Helin, A., Niemi, J.V., Virkkula, A., Pirjola, L., Teinilä, K., Backman, J., Aurela, M., Saarikoski, S., Rönkkö, T., Asmi, E., Timonen, H., 2018. Characteristics and source apportionment of black carbon in the Helsinki metropolitan area, Finland. Atmos. Environ. 190, 87–98. http://dx.doi.org/10.1016/j.atmosenv.2018.07.022, URL: https://www.sciencedirect.com/science/article/pii/S1352231018304692.

Herich, H., Hueglin, C., Buchmann, B., 2011. A 2.5 year's source apportionment study of black carbon from wood burning and fossil fuel combustion at urban and rural sites in Switzerland. Atmos. Meas. Tech. 4 (7), 1409–1420. http://dx.doi.org/10.5194/amt-4-1409-2011, URL: https://amt.copernicus.org/articles/4/1409/2011/.

Hersbach, H., Bell, B., Berrisford, P., Hirahara, S., Horányi, A., Muñoz-Sabater, J., Nicolas, J., Peubey, C., Radu, R., Schepers, D., Simmons, A., Soci, C., Abdalla, S., Abellan, X., Balsamo, G., Bechtold, P., Biavati, G., Bidlot, J., Bonavita, M., De Chiara, G., Dahlgren, P., Dee, D., Diamantakis, M., Dragani, R., Flemming, J., Forbes, R., Fuentes, M., Geer, A., Haimberger, L., Healy, S., Hogan, R.J., Hólm, E., Janisková, M., Keeley, S., Laloyaux, P., Lopez, P., Lupu, C., Radnoti, G., de Rosnay, P., Rozum, I., Vamborg, F., Villaume, S., Thépaut, J.-N., 2020. The ERA5 global reanalysis. Q. J. R. Meteorol. Soc. 146 (730), 1999–2049. http://dx.doi.org/10.1002/qj.3803, URL: https://rmets.onlinelibrary.wiley.com/doi/abs/10.1002/qj.3803.

Hirsch, R., Slack, J., Smith, R., 1982. Techniques of trend analysis for monthly water quality data. Water Resour. Res. 18, 107–121. http://dx.doi.org/10.1029/WR018i001p00107.

Järvi, L., Junninen, H., Karppinen, A., Hillamo, R., Virkkula, A., Mäkelä, T., Pakkanen, T., Kulmala, M., 2008. Temporal variations in black carbon concentrations with different time scales in Helsinki during 1996–2005. Atmos. Chem. Phys. 8 (4), 1017–1027. http://dx.doi.org/10.5194/acp-8-1017-2008, URL: https://acp.copernicus.org/articles/8/1017/2008/.

Ji, Z.-M., 2016. Modeling black carbon and its potential radiative effects over the tibetan plateau. Adv. Clim. Chang. Res. 7 (3), 139–144. http://dx.doi.org/10.1016/j.accre.2016.10.002, URL: https://www.sciencedirect.com/science/article/pii/S1674927816300430.

Jing, A., Zhu, B., Wang, H., Yu, X., An, J., Kang, H., 2019. Source apportionment of black carbon in different seasons in the northern suburb of Nanjing, China. Atmos. Environ. 201, 190–200. http://dx.doi.org/10.1016/j.atmosenv.2018.12.060, URL: https://www.sciencedirect.com/science/article/pii/S1352231019300275.

Kang, S., Zhang, Y., Qian, Y., Wang, H., 2020. A review of black carbon in snow and ice and its impact on the cryosphere. Earth-Sci. Rev. 210, 103346. http://dx.doi.org/10.1016/j.earscirev.2020.103346, URL: https://www.sciencedirect.com/science/article/pii/S0012825220303925.

Kendall, M.G., 1975. Rank Correlation Methods, fourth ed. Charles Griffin, London.

Lack, D., Moosmuller, H., McMeeking, G., Chakrabarty, R., Baumgardner, D., 2013. Characterizing elemental, equivalent black, and refractory black carbon aerosol particles: A review of techniques, their limitations and uncertainties. Anal. Bioanal. Chem. 406, http://dx.doi.org/10.1007/s00216-013-7402-3.

Lee, W.-L., Liou, K., He, C., Liang, H.-C., Wang, T.-C., Li, Q., Liu, Z., Yue, Q., 2017. Impact of absorbing aerosol deposition on snow albedo reduction over the southern Tibetan plateau based on satellite observations. Theor. Appl. Climatol. 129, 1373–1382.

Ljungman, P.L., Andersson, N., Stockfelt, L., Andersson, E.M., Nilsson Sommar, J., Eneroth, K., Gidhagen, L., Johansson, C., Lager, A., Leander, K., et al., 2019. Long-term exposure to particulate air pollution, black carbon, and their source components in relation to ischemic heart disease and stroke. Environ. Health Perspect. 127 (10), 107012. http://dx.doi.org/10.1289/EHP4757.

Luoma, K., Niemi, J.V., Aurela, M., Fung, P.L., Helin, A., Hussein, T., Kangas, L., Kousa, A., Rönkkö, T., Timonen, H., Virkkula, A., Petäjä, T., 2021. Spatiotemporal variation and trends in equivalent black carbon in the helsinki metropolitan area in Finland. Atmos. Chem. Phys. 21 (2), 1173–1189. http://dx.doi.org/10.5194/acp-21-1173-2021, URL: https://acp.copernicus.org/articles/21/1173/2021/.

Mann, H.B., 1945. Nonparametric tests against trend. Econometrica 13 (3), 245–259, URL: http://www.jstor.org/stable/1907187.

Marín, J.C., Raga, G.B., Arévalo, J., Baumgardner, D., Córdova, A.M., Pozo, D., Calvo, A., Castro, A., Fraile, R., Sorribas, M., 2017. Properties of particulate pollution in the port city of Valparaiso, Chile. Atmos. Environ. 171, 301–316. http://dx.doi.org/10.1016/j.atmosenv.2017.09.044.

Matos, V., Estellés, V., Camarasa, J., Sorribas, M., Utrillas, M.P., 2025. Characterization of equivalent black carbon (eBC) in different environments in the western Mediterranean. Atmospheric Pollut. Res. 16 (2), 102367. http://dx.doi.org/10.1016/j.apr.2024.102367.

Mbengue, S., Serfozo, N., Schwarz, J., Ziková, N., Šmejkalová, A.H., Holoubek, I., 2020. Characterization of equivalent black carbon at a regional background site in Central Europe: Variability and source apportionment. Environ. Pollut. 260, 113771. http://dx.doi.org/10.1016/j.envpol.2019.113771, URL: https://www.sciencedirect.com/science/article/pii/S0269749119328477.

Mousavi, A., Sowlat, M.H., Hasheminassab, S., Polidori, A., Sioutas, C., 2018. Spatio-temporal trends and source apportionment of fossil fuel and biomass burning black carbon (BC) in the Los Angeles Basin. Sci. Total Environ. 640–641, 1231–1240. http://dx.doi.org/10.1016/j.scitotenv.2018.06.022.

Mousavi, A., Sowlat, M.H., Lovett, C., Rauber, M., Szidat, S., Boffi, R., Borgini, A., De Marco, C., Ruprecht, A.A., Sioutas, C., 2019. Source apportionment of black carbon (BC) from fossil fuel and biomass burning in metropolitan Milan, Italy. Atmos. Environ. 203, 252–261. http://dx.doi.org/10.1016/j.atmosenv.2019.02.009, URL: https://www.sciencedirect.com/science/article/pii/S1352231019301013.

Petzold, A., Ogren, J.A., Fiebig, M., Laj, P., Li, S.-M., Baltensperger, U., Holzer-Popp, T., Kinne, S., Pappalardo, G., Sugimoto, N., Wehrli, C., Wiedensohler, A., Zhang, X.-Y., 2013. Recommendations for reporting "black carbon" measurements. Atmos. Chem. Phys. 13 (16), 8365–8379. http://dx.doi.org/10.5194/acp-13-8365-2013, URL: https://acp.copernicus.org/articles/13/8365/2013/.

Sandradewi, J., Prevot, A., Szidat, S., Perron, N., Alfarra, M., Lanz, V., Weingartner, E., Baltensperger, U., 2008a. Using aerosol light absorption measurements for the quantitative determination of wood burning and traffic emission contributions to particulate matter. Environ. Sci. Technol. 42, 3316–3323. http://dx.doi.org/10.1021/es702253m.

Sandradewi, J., Prévôt, A., Weingartner, E., Schmidhauser, R., Gysel, M., Baltensperger, U., 2008b. A study of wood burning and traffic aerosols in an alpine valley using a multi-wavelength aethalometer. Atmos. Environ. 42 (1), 101–112. http://dx.doi.org/10.1016/j.atmosenv.2007.09.034, url=https://www.sciencedirect.com/science/article/pii/S1352231007008072.

Savadkoohi, M., Pandolfi, M., Favez, O., Putaud, J.-P., Eleftheriadis, K., Fiebig, M., Hopke, P.K., Laj, P., Wiedensohler, A., Alados-Arboledas, L., Bastian, S., Chazeau, B., María, Á.C., Colombi, C., Costabile, F., Green, D.C., Hueglin, C., Liakakou, E., Luoma, K., Listrani, S., Mihalopoulos, N., Marchand, N., Močnik, G., Niemi, J.V., Ondráček, J., Petit, J.-E., Rattigan, O.V., Reche, C., Timonen, H., Titos, G., Tremper, A.H., Vratolis, S., Vodička, P., Funes, E.Y., zda Zíková, N., Harrison, R.M., Petäjä, T., Alastuey, A., Querol, X., 2024. Recommendations for reporting equivalent black carbon (eBC) mass concentrations based on long-term pan-European in-situ observations. Environ. Int. 185, 108553. http://dx.doi.org/10.1016/j.envint.2024.108553, URL: https://www.sciencedirect.com/science/article/pii/S0160412024001399.

Savadkoohi, M., Pandolfi, M., Reche, C., Niemi, J.V., Mooibroek, D., Titos, G., Green, D.C., Tremper, A.H., Hueglin, C., Liakakou, E., Mihalopoulos, N., Stavroulas, I., Artiñano, B., Coz, E., Alados-Arboledas, L., Beddows, D., Riffault, V., De Brito, J.F., Bastian, S., Baudic, A., Colombi, C., Costabile, F., Chazeau, B., Marchand, N., Gómez-Amo, J.L., Estellés, V., Matos, V., van der Gaag, E., Gille, G., Luoma, K., Manninen, H.E., Norman, M., Silvergren, S., Petit, J.-E., Putaud, J.-P., Rattigan, O.V., Timonen, H., Tuch, T., Merkel, M., Weinhold, K., Vratolis, S., Vasilescu, J., Favez, O., Harrison, R.M., Laj, P., Wiedensohler, A., Hopke, P.K., Petäjä, T., Alastuey, A., Querol, X., 2023. The variability of mass concentrations and source apportionment analysis of equivalent black carbon across urban Europe. Environ. Int. 178, 108081. http://dx.doi.org/10.1016/j.envint.2023.108081, URL: https://www.sciencedirect.com/science/article/pii/S0160412023003549.

Schmid, O., Artaxo, P., Arnott, W.P., Chand, D., Gatti, L.V., Frank, G.P., Hoffer, A., Schnaiter, M., Andreae, M.O., 2006. Spectral light absorption by ambient aerosols influenced by biomass burning in the amazon basin. I: Comparison and field calibration of absorption measurement techniques. Atmos. Chem. Phys. 6 (11), 3443–3462. http://dx.doi.org/10.5194/acp-6-3443-2006, URL: https://acp.copernicus.org/articles/6/3443/2006/.

Segura, S., Estellés, V., Esteve, A., Marcos, C., Utrillas, M., Martínez-Lozano, J., 2016. Multiyear in-situ measurements of atmospheric aerosol absorption properties at an urban coastal site in western Mediterranean. Atmos. Environ. 129, 18–26. http://dx.doi.org/10.1016/j.atmosenv.2016.01.008, URL: https://www.sciencedirect.com/science/article/pii/S1352231016300085.

Segura, S., Estellés, V., Titos, G., Lyamani, H., Utrillas, M.P., Zotter, P., Prèvôt, A.S.H., Močnik, G., Alados-Arboledas, L., Martínez-Lozano, J.A., 2014. Determination and analysis of in situ spectral aerosol optical properties by a multi-instrumental approach. Atmos. Meas. Tech. 7 (8), 2373–2387. http://dx.doi.org/10.5194/amt-7-2373-2014, URL: https://amt.copernicus.org/articles/7/2373/2014/.

Sen, P.K., 1968. Estimates of the regression coefficient based on Kendall's tau. J. Amer. Statist. Assoc. 63 (324), 1379–1389. http://dx.doi.org/10.1080/01621459.1968.10480934.

Shen, L., Wang, H., Kong, X., Zhang, C., Shi, S., Zhu, B., 2021. Characterization of black carbon aerosol in the Yangtze River Delta, China: Seasonal variation and source apportionment. Atmos. Pollut. Res. 12 (1), 195–209. http://dx.doi.org/10.1016/j.apr.2020.08.035, URL: https://www.sciencedirect.com/science/article/pii/S1309104220302634.

Sicard, P., Agathokleous, E., Paoletti, E., Calatayud, V., 2021. Urban population exposure to air pollution in Europe over the last decades. Environ. Sci. Eur. 33, http://dx.doi.org/10.1186/s12302-020-00450-2.

Sun, J., Birmili, W., Hermann, M., Tuch, T., Weinhold, K., Merkel, M., Rasch, F., Müller, T., Schladitz, A., Bastian, S., Löschau, G., Cyrys, J., Gu, J., Flentje, H., Briel, B., Asbach, C., Kaminski, H., Ries, L., Sohmer, R., Gerwig, H., Wirtz, K., Meinhardt, F., Schwerin, A., Bath, O., Ma, N., Wiedensohler, A., 2020. Decreasing trends of particle number and black carbon mass concentrations at 16 observational sites in Germany from 2009 to 2018. Atmos. Chem. Phys. 20 (11), 7049–7068. http://dx.doi.org/10.5194/acp-20-7049-2020.

Theil, H., 1950. A rank invariant method of linear and polynomial regression analysis, i, ii, iii.. In: Proceedings of the Koninklijke Nederlandse Akademie Wetenschappen, Series a Mathematical Sciences. Vol. 53, pp. 386–392, 521–525, 1397–1412.

Titos, G., del Águila, A., Cazorla, A., Lyamani, H., Casquero-Vera, J., Colombi, C., Cuccia, E., Gianelle, V., Močnik, G., Alastuey, A., Olmo, F., Alados-Arboledas, L., 2017. Spatial and temporal variability of carbonaceous aerosols: Assessing the impact of biomass burning in the urban environment. Sci. Total Environ. 578, 613–625. http://dx.doi.org/10.1016/j.scitotenv.2016.11.007, URL: https://www.sciencedirect.com/science/article/pii/S004896971632438X.

Tiwari, S., Pipal, A., Srivastava, A., Bisht, D., Pandithura, G., 2014. Determination of wood burning and fossil fuel contribution of black carbon at Delhi, India using aerosol light absorption technique. Environ. Sci. Pollut. Res. 22, 2846–2855. http://dx.doi.org/10.1007/s11356-014-3531-2.

Virkkula, A., Mäkelä, T., Hillamo, R., Yli-Tuomi, T., Hirsikko, A., Hämeri, K., Koponen, I.K., 2007. A simple procedure for correcting loading effects of aethalometer data. J. Air Waste Manage. Assoc. 57 (10), 1214–1222. http://dx.doi.org/10.3155/1047-3289.57.10.1214, arXiv:https://doi.org/10.3155/1047-3289.57.10.1214.

Weingartner, E., Saathoff, H., Schnaiter, M., Streit, N., Bitnar, B., Baltensperger, U., 2003. Absorption of light by soot particles: determination of the absorption coefficient by means of aethalometers. J. Aerosol Sci. 34 (10), 1445–1463. http://dx.doi.org/10.1016/S0021-8502(03)00359-8.

WHO, 2013. Review of the Evidence on Health Aspects of Air Pollution - REVIHAAP. Technical Report, World Health Organization, Copenhagen.

WHO, 2021. WHO Global Air Quality Guidelines. particulate Matter ($PM_{2.5}$ and PM_{10}), Ozone, Nitrogen Dioxide, Sulfur Dioxide and Carbon Monoxide. World Health Organization, Geneva.

Yue, S., Pilon, P., Phinney, B., Cavadias, G., 2002. The influence of autocorrelation on the ability to detect trend in hydrological series. Hydrol. Process. 16 (9), 1807–1829. http://dx.doi.org/10.1002/hyp.1095.

Yus-Díez, J., Via, M., Alastuey, A., Karanasiou, A., Minguillón, M.C., Perez, N., Querol, X., Reche, C., Ivančič, M., Rigler, M., Pandolfi, M., 2022. Absorption enhancement of black carbon particles in a Mediterranean city and countryside: effect of particulate matter chemistry, ageing and trend analysis. Atmos. Chem. Phys. 22 (13), 8439–8456. http://dx.doi.org/10.5194/acp-22-8439-2022, URL: https://acp.copernicus.org/articles/22/8439/2022/.

Zanatta, M., Gysel, M., Bukowiecki, N., Müller, T., Weingartner, E., Areskoug, H., Fiebig, M., Yttri, K., Mihalopoulos, N., Kouvarakis, G., Beddows, D., Harrison, R., Cavalli, F., Putaud, J., Spindler, G., Wiedensohler, A., Alastuey, A., Pandolfi, M., Sellegri, K., Swietlicki, E., Jaffrezo, J., Baltensperger, U., Laj, P., 2016. A European aerosol phenomenology-5: Climatology of black carbon optical properties at 9 regional background sites across europe. Atmos. Environ. 145, 346–364. http://dx.doi.org/10.1016/j.atmosenv.2016.09.035, URL: https://www.sciencedirect.com/science/article/pii/S135223101630735X.

Zotter, P., Herich, H., Gysel, M., El-Haddad, I., Zhang, Y., Močnik, G., Hüglin, C., Baltensperger, U., Szidat, S., Prévôt, A.S.H., 2017. Evaluation of the absorption ångström exponents for traffic and wood burning in the aethalometer-based source apportionment using radiocarbon measurements of ambient aerosol. Atmos. Chem. Phys. 17 (6), 4229–4249. http://dx.doi.org/10.5194/acp-17-4229-2017.